Supplementary Information (SI) for Journal of Materials Chemistry B.

SUPPORTING INFORMATION

Donor-acceptor squaraine based theranostic platforms for combined type I photodynamic, photothermal and chemo therapies

Melek Pamuk Algi [a,*] , Donay Cungur [b]

[a] *Department of Chemistry & ASUBTAM M. Bilmez BioNanoTech Lab., Aksaray University, TR-68100 Aksaray, Turkey.*

[b] *Department of Nanotechnology & ASUBTAM M. Bilmez BioNanoTech Lab., Aksaray University, TR-68100 Aksaray, Turkey.*

Corresponding author e-mail: melekalgi@gmail.com (M. P. ALGI)

General Methods

All chemicals were purchased from Sigma-Aldrich or Merck and used without further purification unless otherwise stated. Column chromatography was performed using silica gel (60–200 mesh) from Merck. Thin-layer chromatography (TLC) was conducted on Merck 0.2 mm silica gel 60 F_{254} analytical aluminum plates. Nuclear magnetic resonance (NMR) spectra were recorded on a Bruker Ultrashield 300 spectrometer at 600 MHz for ^{1}H and 151 MHz for ^{13}C. Fourier-transform infrared (FTIR) spectra were obtained using a Thermo Scientific Nicolet iS5 spectrometer equipped with an iD5-ATR accessory. UV-Vis absorption and fluorescence spectra were measured using Varian Cary 50 and Varian Cary Eclipse spectrophotometers, respectively. High-resolution mass spectrometry (HRMS) measurements were carried out using a Thermo Scientific TSQ Quantum Access Max spectrometer. 1 Watt 635 nm laser Oxlasers used. Thermal monitoring was performed with HIKMICRO Handheld Thermography Cameras.

NIR laser-induced PTT

Squaraine 9 solutions were exposed to near-infrared (NIR) laser irradiation (635 nm, Oxlasers) at a power density of 1 W/cm² for 10 minutes. Real-time thermal imaging was conducted using a HIKMICRO Handheld Thermography Cameras thermal camera to monitor temperature variations. The photothermal conversion efficiency (η) was calculated based on Equation 2.

$$\eta \frac{\Sigma miCp,i\,(\Delta T_s - \Delta T_B)}{\tau_s \quad P(1-10^{-A})} \qquad (2)$$

Preparation of cells

Cell preparation procedures were carried out in a sterile environment within a laminar flow cabinet using established protocols from the literature (Bonifacino et al., 2001). In this study, SK-MEL-30 (DSMZ No.: ACC 151) and MCF-7 (ATCC® HTB-22™) were used as cancer cell lines, while L929 (ATCC® CRL-6364™) fibroblast cells served as the healthy control. These cells were incubated in their respective culture media at 37 °C under a 5% CO_2 atmosphere. Once the cells reached 70–80% confluence, they were passaged through trypsinization. Depending on the analyses to be performed, cells were seeded into well plates and prepared for subsequent experiments.

Biocompatibility Test

Cells were added to 96-well plates and incubated until the concentration or storage was recorded when the logarithmic phase was reached. During the incubation period (24 hours), the medium was washed and fresh medium was applied to the wells and MTT solution (11 µl) was added. At the end of the 3-hour incubation at 37 °C, the medium was removed and DMSO was added.[1] Percent viability was calculated by reading the absorbance values in the microplate reader.[2] Cell viability was calculated with the formula Rv=((A1−A0) / (A2−A0)) ×100%. Rv cell viability, A0 blank control group absorbance, A1 group absorbance, A2 control group absorbance.[3-4]

Cell Viability Assay

For bioimaging studies, cells were seeded into Petri dishes and allowed to grow until they reached 50–70% confluence. The culture medium was then removed, and the cells were washed three times with PBS. Subsequently, they were incubated in a dye-containing medium at 37 °C under a 5% CO_2 atmosphere for 24 hours. After incubation, excess dye was removed by washing with PBS. The cells were then fixed by incubating them in a 3.7% formaldehyde-PBS solution

for 10 minutes. Finally, DAPI was added, and after 40 minutes of incubation, the cells were visualized using a fluorescence microscope.

Fluorescence Quantum Yield of Squaraine 9

The desired fluorescence quantum yield for Squaraine **9** was measured against methylene blue[10] with a reported quantum yield of 0.02. The fluorescence quantum yield (Φ) was determined using the correlation between the absorbance (A) at the excitation wavelength of the compounds and the integrated fluorescence intensity (F) as per the equation (1) provided below.[11]

$$\Phi_x(\lambda) = \Phi_{st}(\lambda) \times F_x/F_{st} \times A_{st}(\lambda)/A_x(\lambda) \times h_x^2/h_{st}^2 \quad (1)$$

The subscripts st and x in the formula denote the standard and sample, respectively. η represents the refractive indices of the solvent.

Statistical Analysis

Data analysis was conducted using GraphPad Prism 8.0 software. The test findings were presented as mean ± standard error, utilizing two-way ANOVA followed by

Bonferroni post hoc analysis. ****P<0.0001 (n=3). Data are presented as the averages of three independent experiments.

Spectral Data

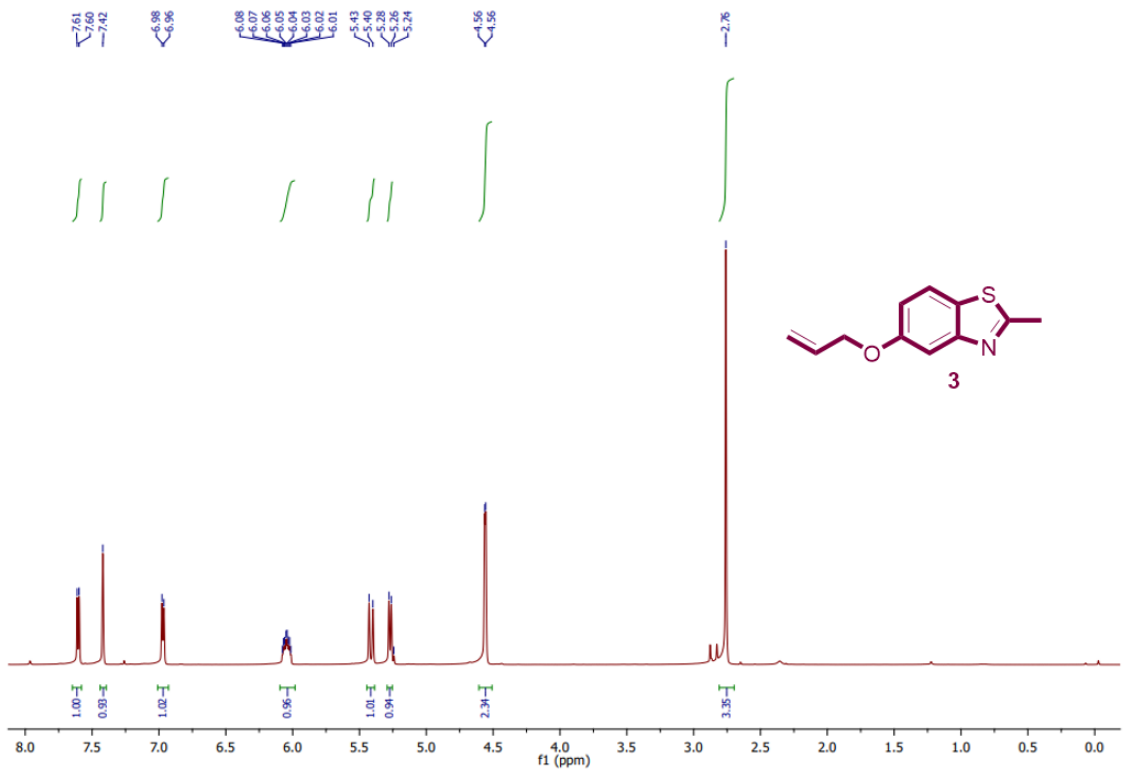

Fig S1. ^{1}H NMR spectrum for compound **3** ($CDCl_3$, 600 MHz).

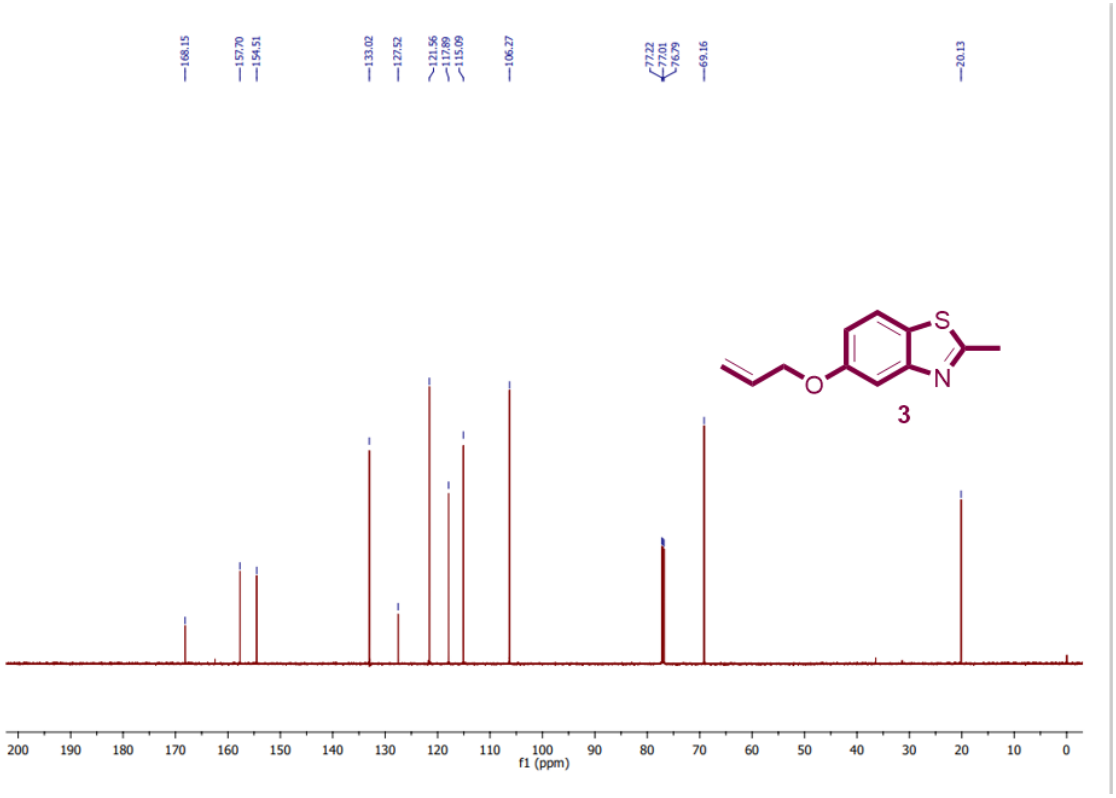

Fig S2. ^{13}C NMR spectrum for compound **3** ($CDCl_3$, 151 MHz).

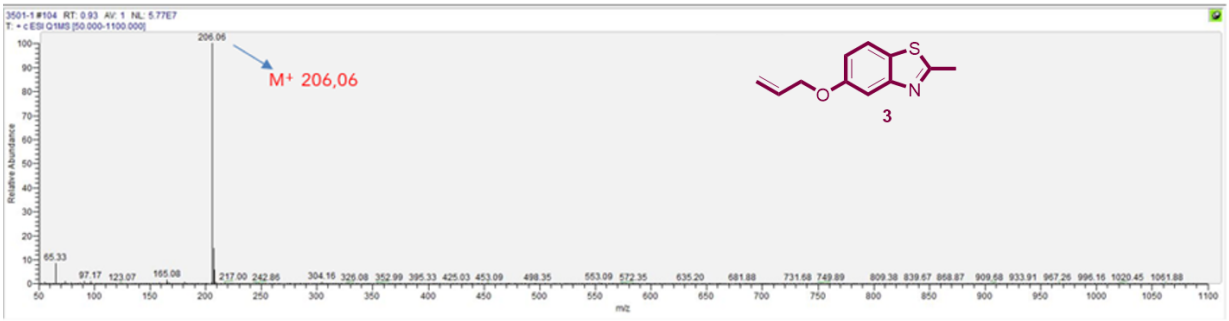

Fig S3. LC-MS mass spectrum for compound **3**.

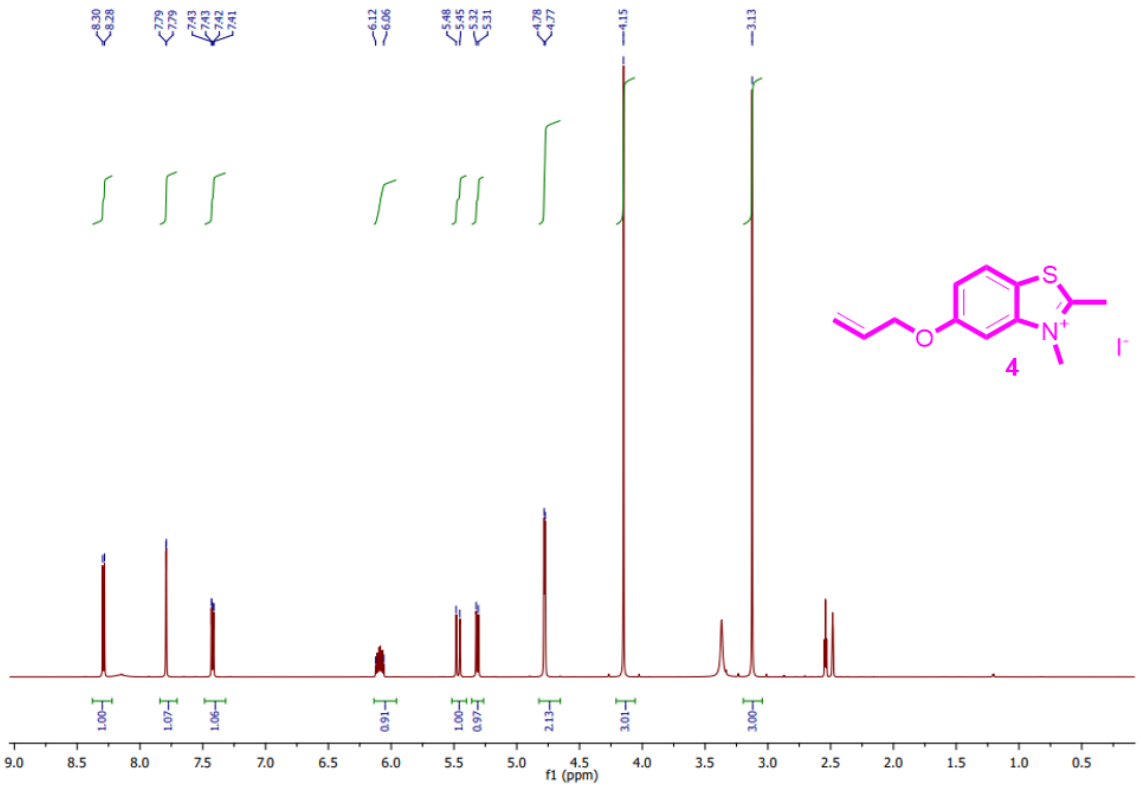

Fig S4. ^{1}H NMR spectrum for indoline **4** (DMSO-d_6, 600 MHz).

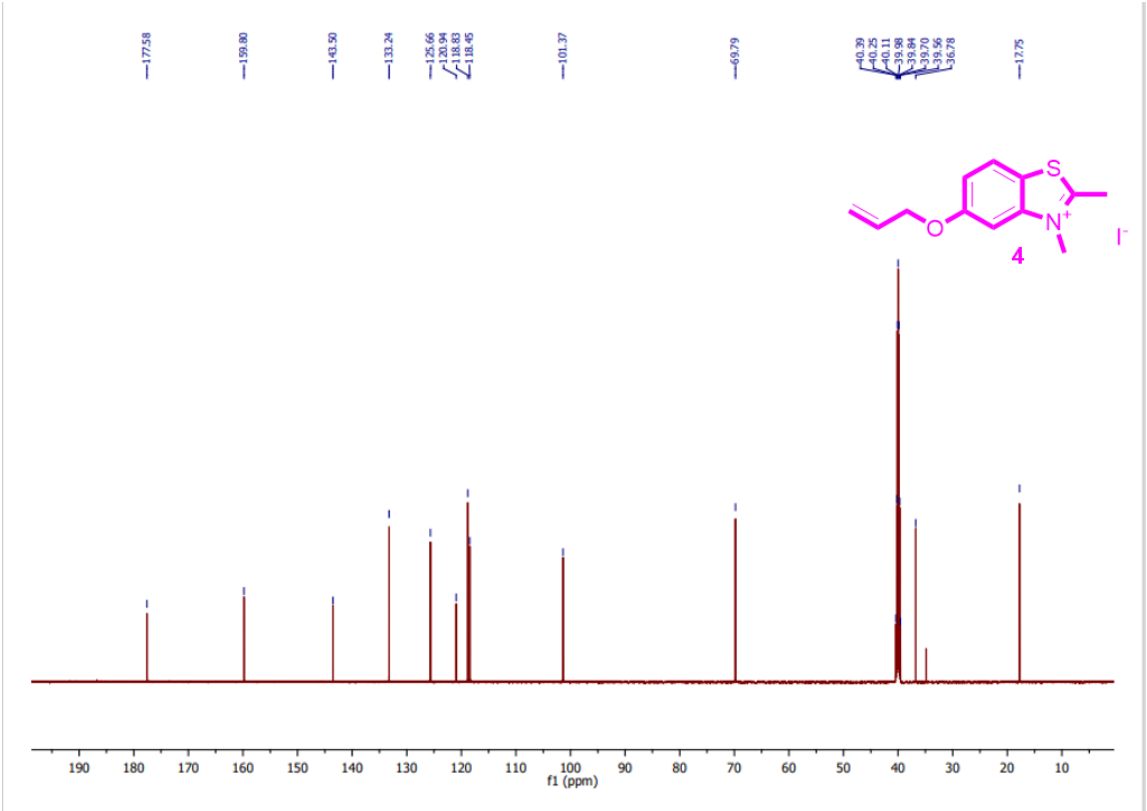

Fig S5. ^{13}C NMR spectrum for indoline **4** (DMSO-d_6, 151 MHz).

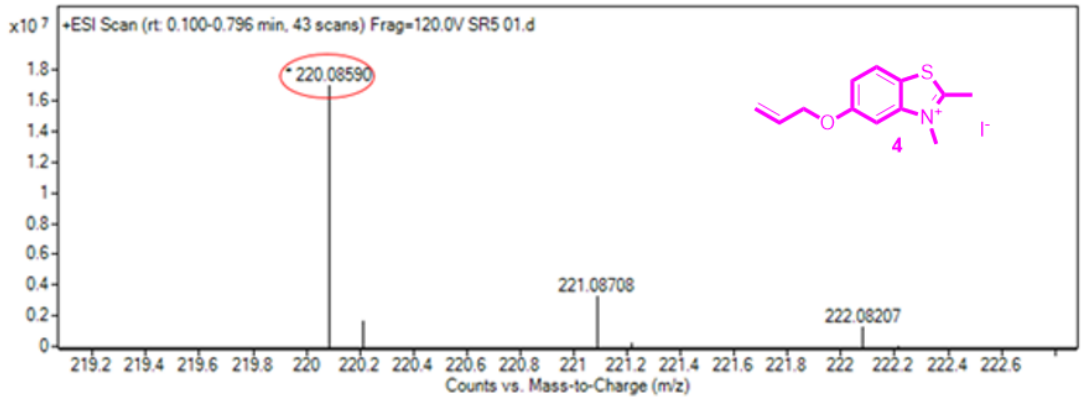

Fig S6. Mass spectrum for indoline 4.

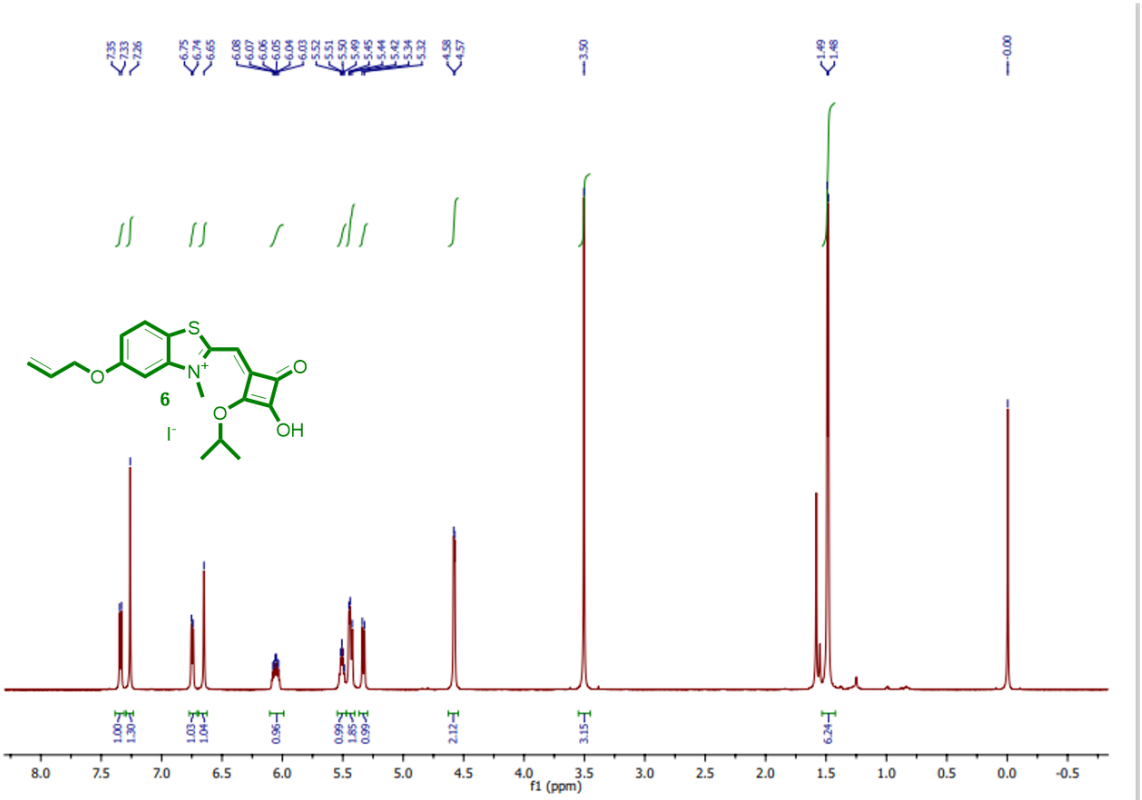

Fig S7. ^{1}H NMR spectrum for compound **6** ($CDCl_3$, 600 MHz).

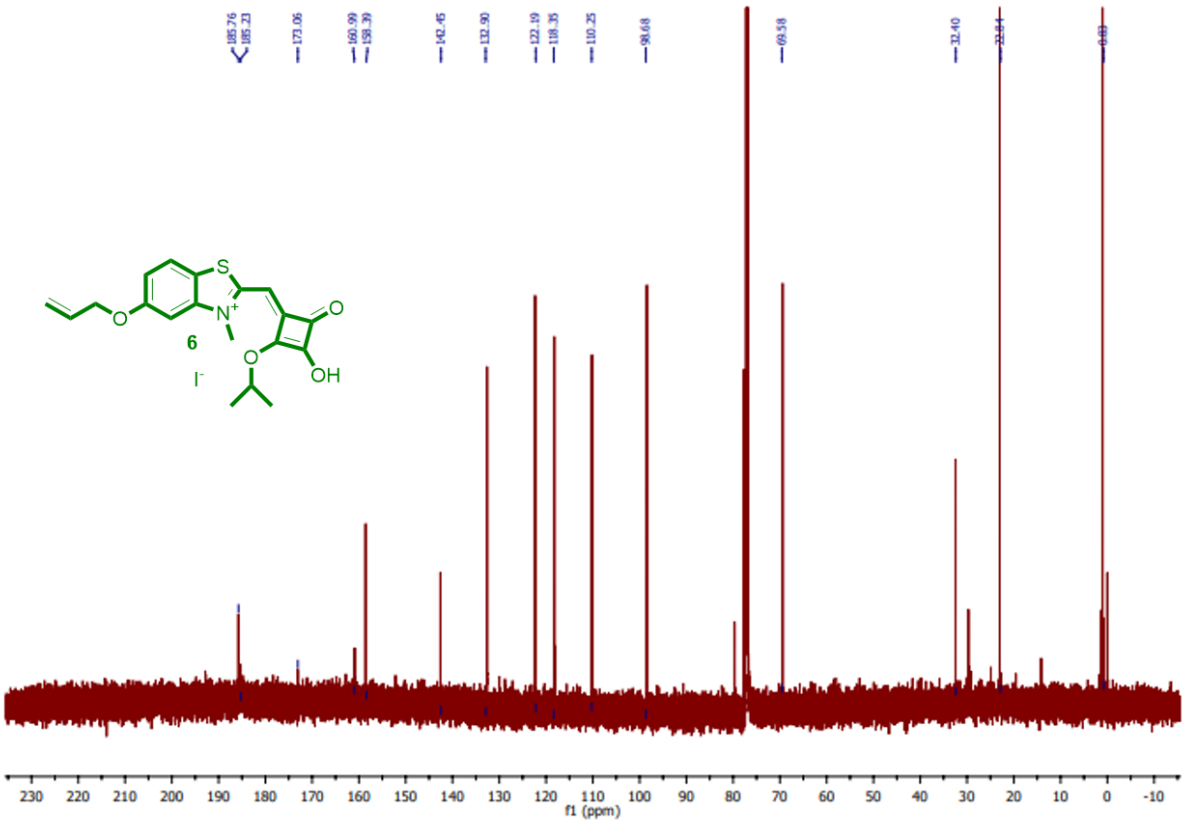

Fig S8. ^{13}C NMR spectrum for Compound **6** ($CDCl_3$, 151 MHz).

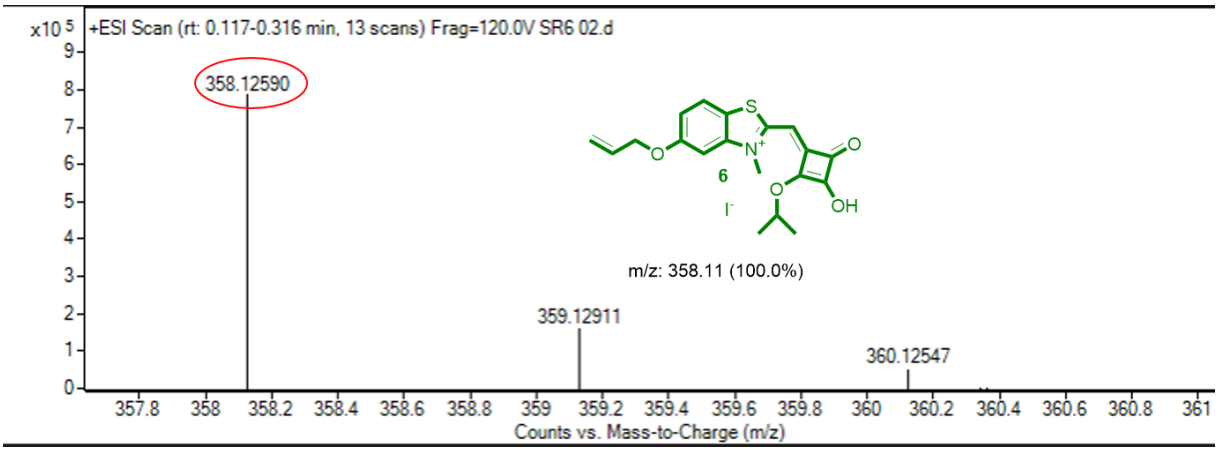

Fig S9. Mass spectrum for compound **6**.

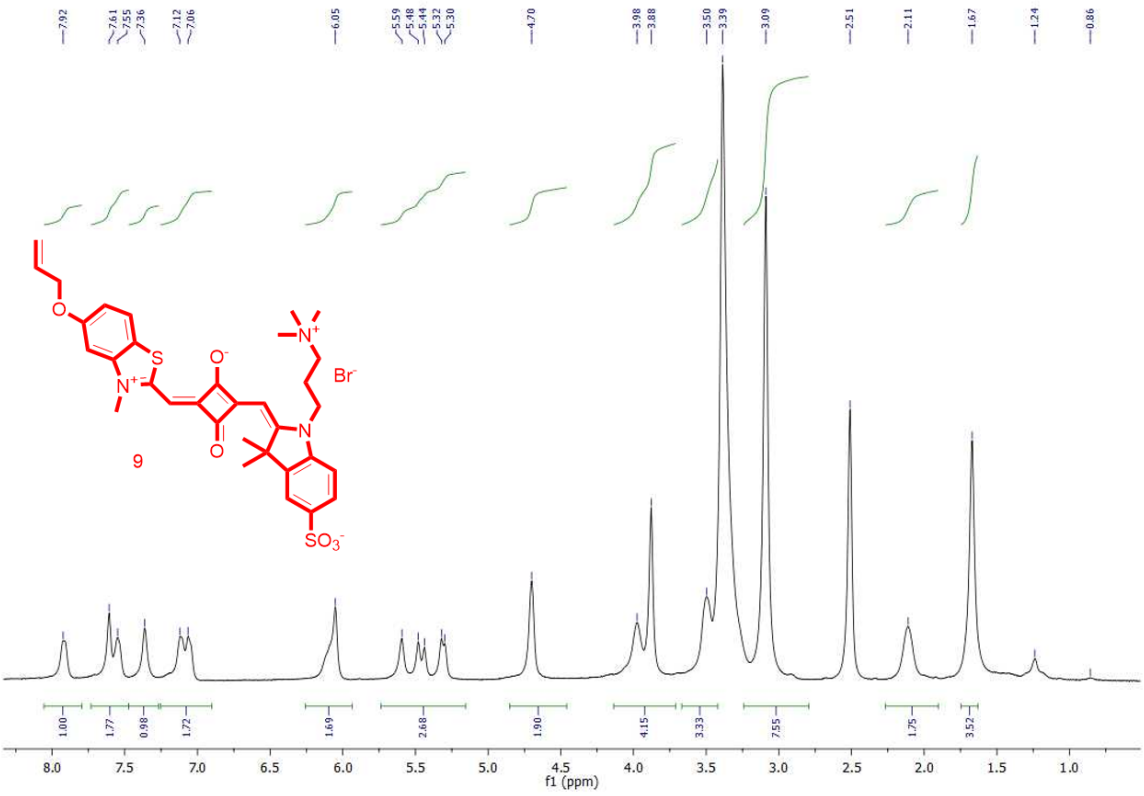

Fig S10. ^{1}H NMR spectrum for squaraine **9** (DMSO-d_6, 600 MHz).

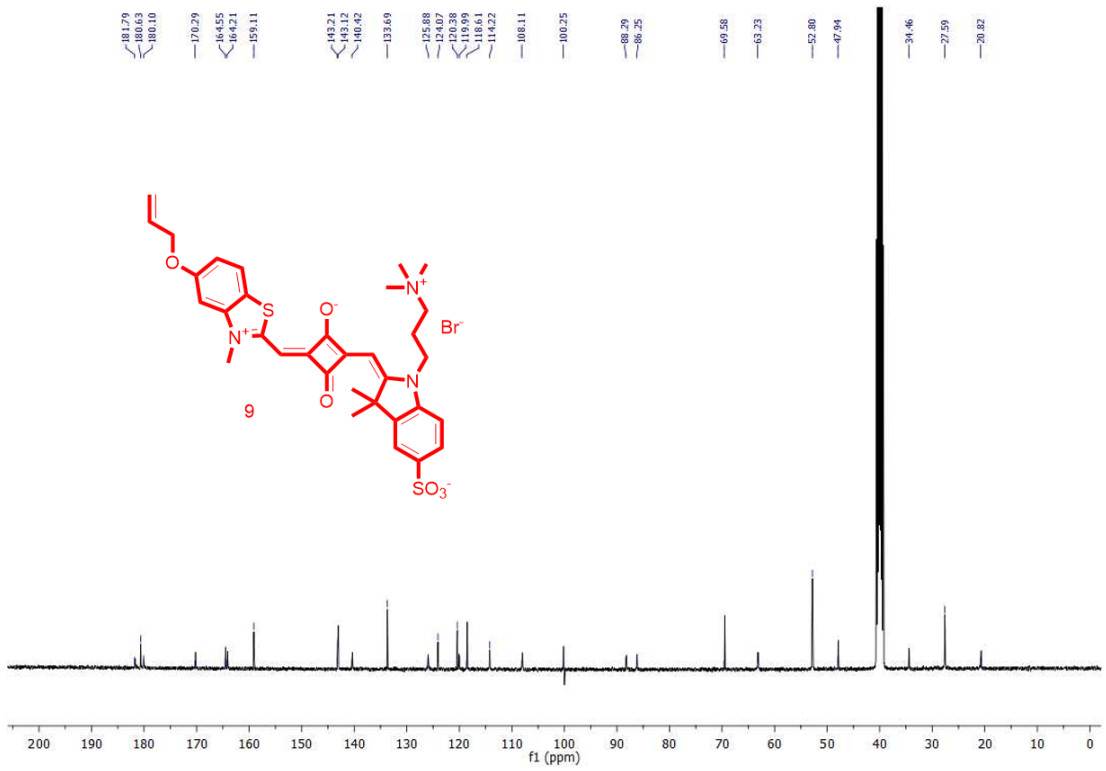

Fig S11. ^{13}C NMR spectrum for squaraine **9** (DMSO-d_6, 150 MHz).

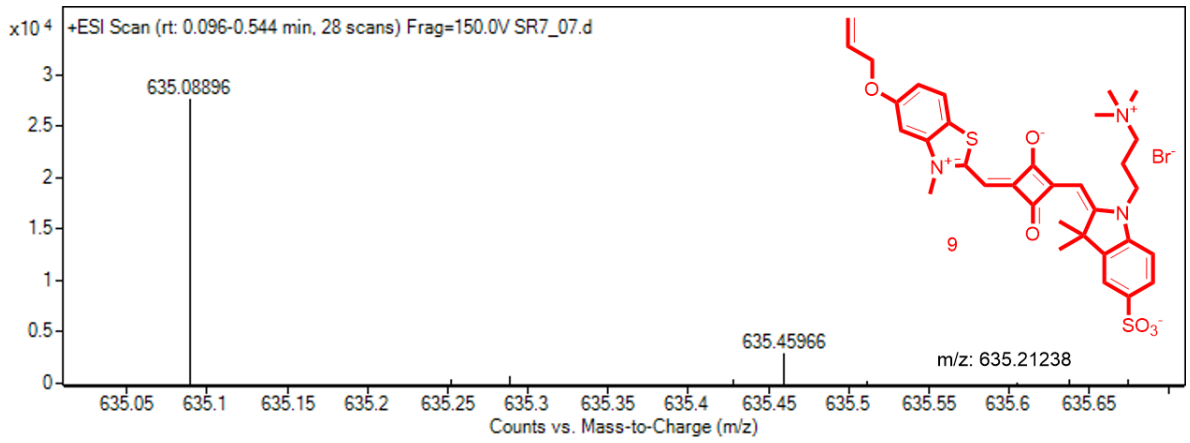

Fig S12. HRMS spectrum for squaraine **9**.

General Procedure for Synthesis of Squaraine 9@PA

Acrylamide (AAm) (250 mg, 3.517 mmol), Squarine 9 (2.5-5.0-7.5 mg), and N,N'-Methylenebisacrylamide (MBA) (1.0 mg, 0.0065 mmol) were weighed into a 15 mL vial. Then, 0.5 mL of deionized water was added, and the mixture was stirred under a nitrogen atmosphere. Ammonium persulfate (APS) (5 mg, 0.021 mmol) was added, and the prepared solution was transferred into 1 mL syringes and placed in an oven set at 65°C until hydrogel formation was observed (24 hours). Afterward, the hydrogels were placed in water, and their swelling was monitored by changing the water at specific time intervals. The mass of the hydrogels was measured after changing the water, and the swelling ratio was calculated using the formula provided above. The equilibrated hydrogels were then freeze-dried.

FTIR of $9_{2.5}$@PA (cm^{-1}): 3335, 3185, 2942, 2360, 1651, 1607, 1448, 1417, 1318, 1121.

FTIR of $9_{5.0}$@PA (cm^{-1}): 3335, 3186, 2934, 1647, 1604, 1448, 1417, 1320, 1122.

FTIR of $9_{7.5}$@PA (cm^{-1}): 3336, 3190, 2937, 1662, 1608, 1448, 1417, 1318, 1122.

Quantitative ROS comparison between normoxic and hypoxic environments

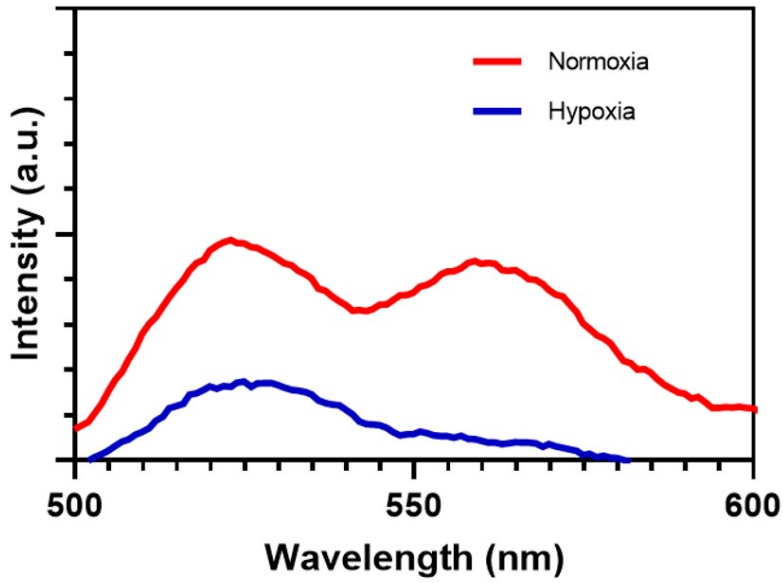

Fig S13. Quantitative ROS comparison between hypoxic (blue, total peak area: 256.4) and normoxic (red, total peak area: 427.6) environments.

The uptake of Squaraine 9 by cancer cells

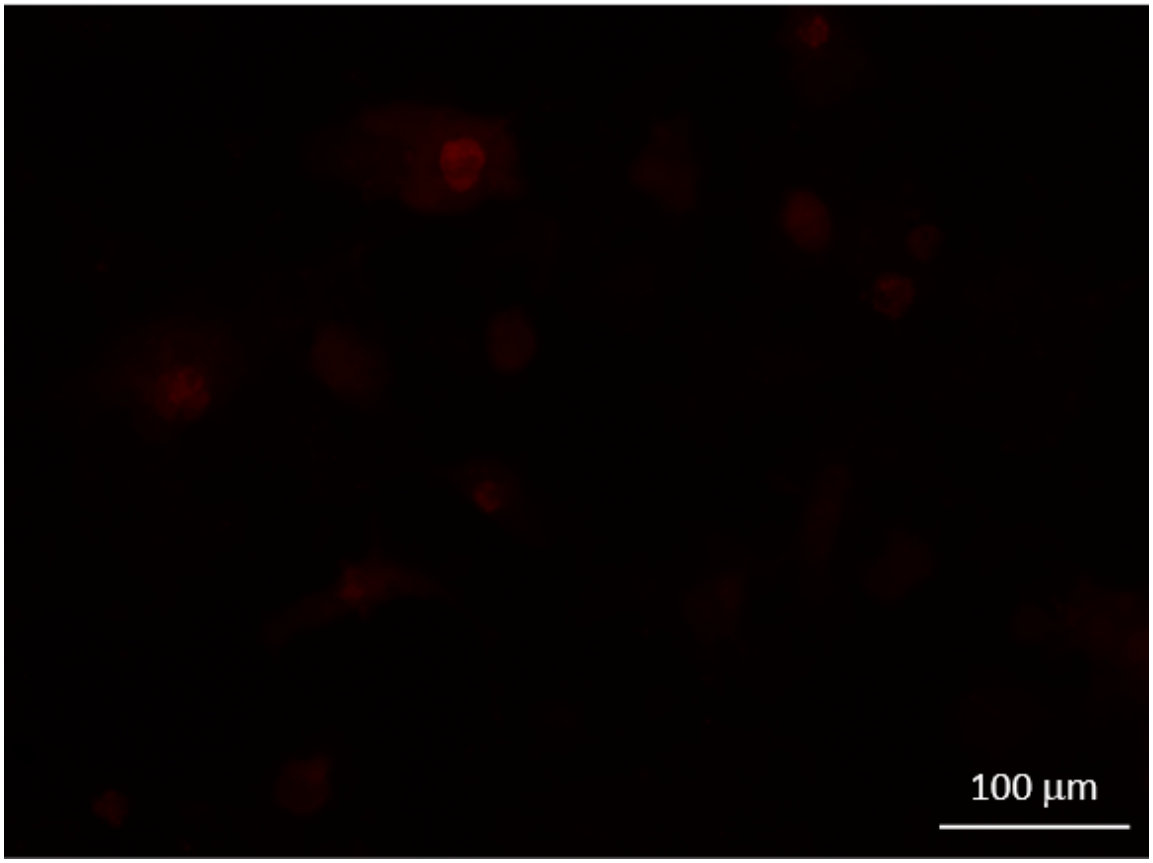

Fig S14. Fluorescence microscopy image of squaraine **9**, which is cell-permeable and efficiently internalized by cancer cells after two hours of post incubation, facilitating effective fluorescence imaging of SK-MEL-30 cancer cells.

Drug Release Profiles of Squaraine 9@PA Hydrogels

The release kinetics were evaluated using the Korsmeyer–Peppas model to elucidate the release mechanism under laser irradiation and dark conditions. The model is expressed as:

$Q = k \cdot t^n$

For linearization, the logarithmic form was used:

$$log Q = log k + n log t$$

where *Q* is the cumulative release, *k* is the release rate constant, and *n* is the release exponent indicating the mechanism of transport. To ensure the validity of the model, only the initial ~60% release region (0–16 min) was considered.

Under laser irradiation, the slope of the log–log plot yielded an *n* value of approximately 0.72 (R^2 = 0.9692). In contrast, under dark conditions, the calculated *n* value was approximately 0.08, indicating a negligible release contribution and a highly restricted diffusion process.[5]

Mechanical properties of PA and Squaraine 9@PA Hydrogels

The compression tests were done to find out the strength of hydrogels. The swelling and the presence of **9** had a clear effect on how the hydrogels behaved mechanically (Figure S14). The strongest compressive strength was found in dry hydrogels (PA hydrogels) and hydrogels without **9**. These had a denser and more rigid polymer network. But swollen PA hydrogels (wet) were not as strong. This phenomenon is probably because water makes the polymer chains less strong and more flexible. The hydrogel samples with squaraine (Sq@PA) were weaker than the PA hydrogels, whether dry or swollen. In contrast, hydrogel samples with squaraine (Sq@PA) were weaker mechanically than PA hydrogels, whether they were dry or swollen. It is thought that squaraine lowered the cross-linking density and made the polymer network's structure more varied. The swollen Sq@PA hydrogels were the weakest when it came to compression, but they were also more flexible and ductile, with a wider range of deformation. In conclusion, swelling weakens the hydrogel network, and squaraine dye makes this effect even stronger, which makes the material less strong.

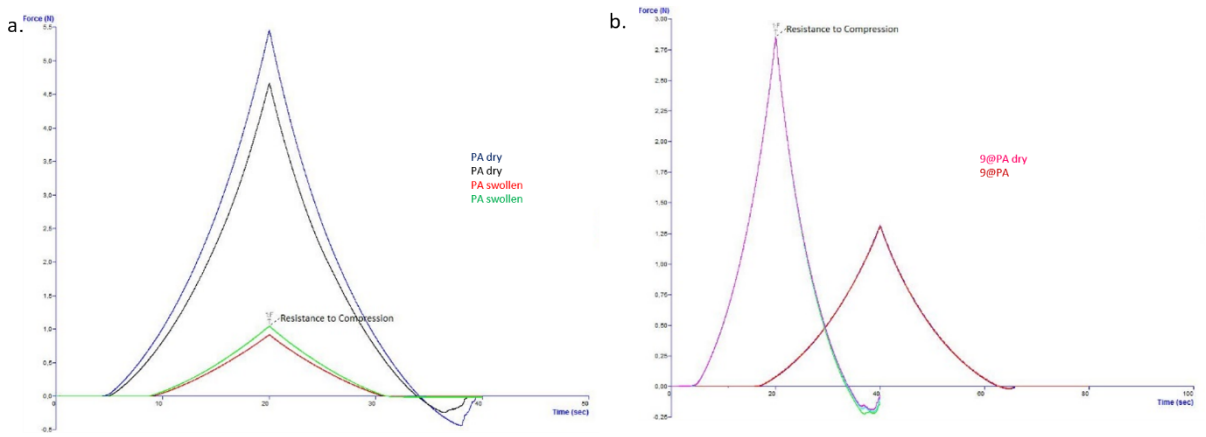

Fig S15. The compression tests results for hydrogels.

References

1. L. Li, W. Zhao, Z. Qu, L. Shi, S. Tan, E. Ha, T. Jia, T. Sun. Novel phthalocyanine-based micelles/PNIPAM composite hydrogels: Spatially/temporally controlled drug release triggered by NIR laser irradiation New Journal of Chemistry. 2020. 44(21), 8705-9.

2. M. Yang, X. Lu, L. Tang, Y. Fu, P. Yang. Thermosensitive nanocomposite gel loaded zinc phthalocyanine for photodynamic therapy, Journal of Polymer Research. 2020. 27(9), 287.

3. A. J. Siddiqa, N. K. Shrivastava, M. E. A. Mohsin, M. H. Abidi, T. A. Shaikh, M. A. El-Meligy. Preparation of letrozole dispersed pHEMA/AAm-g-LDPE drug release system: In-vitro release kinetics for the treatment of endometriosis, Colloids and Surfaces B: Biointerfaces. 2019. 179, 445-52.

4. Y.-Y. Xie, Y.-W. Zhang, X.-Z. Liu, X.-F. Ma, X.-T. Qin, S.-R. Jia, C. Zhong. Aggregation-induced emission-active amino acid/berberine hydrogels with enhanced photodynamic antibacterial and anti-biofilm activity, Chemical Engineering Journal. 2021. 413, 127542.

5. S. Erikci, N. van den Bergh, H. Boehm. (2024). Kinetic and Mechanistic Release Studies on Hyaluronan Hydrogels for Their Potential Use as a pH-Responsive Drug Delivery Device. In *Gels* (Vol. 10, ss. 731).